Solitons as the Early Stage of Quasicondensate Formation during Evaporative Cooling

E. Witkowska,[1] P. Deuar,[1] M. Gajda,[1] and K. Rzążewski[2]

[1]*Institute of Physics, Polish Academy of Sciences, Aleja Lotników, 02-668 Warsaw, Poland*

[2]*Center for Theoretical Physics, Polish Academy of Sciences, Aleja Lotników, 02-668 Warsaw, Poland*

(Received 20 December 2010; published 30 March 2011)

We calculate the evaporative cooling dynamics of trapped one-dimensional Bose-Einstein condensates for parameters leading to a range of condensates and quasicondensates in the final equilibrium state, using the classical fields method. We confirm that solitons are created during the evaporation process by the Kibble-Zurek mechanism, but subsequently dissipate during thermalization. However, their signature remains in the phase coherence length, which is approximately conserved during dissipation in this system.

DOI: 10.1103/PhysRevLett.106.135301 PACS numbers: 67.85.−d, 03.75.Kk, 05.30.Jp

The quasi-one-dimensional (1D) Bose gas in elongated clouds of neutral ultracold atoms [1,2] differs markedly from the Bose-Einstein condensate (BEC) in three-dimensional geometries. One of the most remarkable features is the presence of two characteristic temperatures when the trapped gas is cooled [2]. Below T_c, the lowest mode becomes appreciably occupied [3] but the phase coherence length $l_\phi \propto 1/T$ is smaller than the size of the system. This is called a quasicondensate. Below a second temperature T_ϕ, l_ϕ grows to the size of the cloud, and the state is a true BEC. The phase coherence in these states have been extensively studied both experimentally [4,5] and theoretically [2,3,6–9].

In thermal equilibrium, the variance in phase and one-body density matrix have been calculated [2,6,9,10]. Their short-range behavior gives the phase correlation length l_ϕ near the center of the trap:

$$\rho_1(z, z') = \langle \hat{\Psi}^\dagger(z)\hat{\Psi}(z')\rangle \approx \rho_1(0, 0)e^{-|z-z'|/l_\phi}. \quad (1)$$

In equilibrium, the phase in a single experimental realization varies smoothly over length scales l_ϕ [10].

On the other hand, phase fluctuations have also been predicted from the Kibble-Zurek mechanism [11] (KZM) after the onset of condensation, when the system is far from equilibrium. These fluctuations are seemingly different in nature than those discussed above. During evaporative cooling, phase defects in the form of gray solitons appear when crossing the characteristic temperature T_c. They are born when local condensation occurs faster than distant regions can communicate to agree on a common phase. When the expanding initial phase domains meet, soliton defects form on the interfaces between them. Therefore, during the formation of a condensate the phase experiences sudden jumps at the temporal position of every soliton, and phase domains appear between them of a size equal to the separation between neighboring solitons. A natural question arises whether these preformed domains are somehow related to the phase fluctuations in equilibrium. The aim of this Letter is to show how the phase fluctuations in these two cases are connected. What we find is that the coherence length is conserved during dissipation, so that the final phase fluctuations are the remnant of the initial solitons.

The number of solitons while crossing T_c has been predicted as a function of the quench rate [7]. A calculation where chemical potential was quenched at $T = 0$ demonstrated the KZM for a uniform gas [8]. Here we show that the Kibble-Zurek scaling also applies for a realistic model of evaporative cooling in a trap. We have simulated the nonequilibrium evaporative cooling dynamics to the stationary thermal state using the classical fields method (CFM) [12]. The observations imply that the solitons are indeed the early stage of development of the final phase fluctuations at equilibrium.

We consider a single-species Bose gas in a trap. We use harmonic oscillator units with frequency ω_z. The initial state is generated in a canonical ensemble at a temperature of $k_B T = 360\hbar\omega_z$ [13], well above T_c in the final state. The description of the system in the CFM is in terms of an ensemble of classical field amplitudes $\psi(z)$ evolving under a generalized Gross-Pitaevskii mean-field evolution equation from thermally randomized initial conditions. This is equivalent to a truncated Wigner description [14], but with quantum fluctuations omitted. It is accurate provided spontaneous processes can be neglected and most modes are appreciably occupied. This is the case here. Related models are compared in [15]. The evolution in time is given by

$$i\partial_t \psi(z, t) = [H(z, t) - i\Gamma(z, t)]\psi(z, t), \quad (2)$$

with the Hamiltonian

$$H(z, t) = -\frac{1}{2}\frac{\partial^2}{\partial z^2} + V(z, t) + g_{1D}|\psi(z, t)|^2 \quad (3)$$

including kinetic energy, contact interactions with strength $g_{1D} = 0.31$ (corresponding to $N = 10^4$ ^{87}Rb atoms in a $10 \times 1000 \times 1000$ Hz trap, very similar parameters to recent experiments [16]), and the time-dependent external potential (shown in Fig. 1)

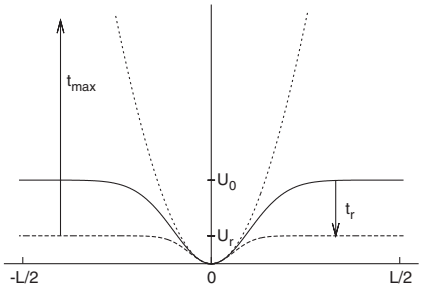

FIG. 1. The evaporative cooling potential $V(z, t)$. Solid line: initially ($t = 0$), dashed line: at the end of the ramp ($t = t_r$), dotted line: during thermal equilibration ($t \gg t_r$).

$$V(z, t) = U(t)[1 - e^{-(z^2/2U(t))}] \tag{4a}$$

$$U(t) = \begin{cases} U_0 + (U_r - U_0)\frac{t}{t_r}, & t \le t_r, \\ U_r + (U_{\max} - U_r)\frac{t - t_r}{t_{\max} - t_r}, & t > t_r. \end{cases} \tag{4b}$$

The first stage ($t < t_r$) is the evaporative cooling ramp. $V(z)$ is a Gaussian dip of constant trap frequency ($\omega_z = 1$ in the units chosen) near $z = 0$, and standard deviation $\sqrt{U(t)}$. The depth of the dip decreases linearly from $U_0 = 100$ to $U_r = U_0/3$. The ramp time t_r is varied to obtain different final states.

After the ramp ($t_r < t < t_{\max}$), the evaporation is stopped and the gas is allowed to thermalize for a longer period to $t_{\max} = t_r + 1000$ in a much deeper potential (rising to a depth $U_{\max} = 10U_0$) that becomes effectively harmonic in the region occupied by the gas cloud. It is also necessary to include losses in the wings of the potential: $\Gamma(z, t) = \Gamma_\infty[V(z, t)/U(t)]^\gamma$ with $\Gamma_\infty = 10$, $\gamma = 50$. This loss acts as a high-energy knife in the region beyond about two (t dependent) standard deviations of the Gaussian dip. This is necessary to realistically model the experimental properties of the trap by preventing once evaporated atoms from returning back. A lattice of 1024 points on a length $L = 120$ is used. The number of trapped atoms we obtain for $t \ge t_r$ is always around $N \approx 1300$. The widths and shapes of the clouds agree very well with the radius $z_{\mathrm{TF}} = \sqrt{2\mu}$ and chemical potential $\mu = [9(g_{1\mathrm{D}}N)^2/32]^{(1/3)}$ predicted by the Thomas-Fermi approximation.

Figure 2 shows the time evolution of a single realization of the experiment in the quasicondensate ($t_r = 75$) and BEC ($t_r = 400$) regimes. Animations for $t_r = 250$ are in [17]. We see the emergence of a great number of defects on the healing-length scale in the early part of the cooling phase [e.g., around $t = 6$–10 in Fig. 2(c)]. The density dips in Figs. 2(a), 2(c), and 2(d) display all the characteristics of gray solitons: passing through each other, turnaround near the edge of the cloud when the central density reaches zero, motion much slower than the speed of sound, phase jumps, and width in agreement with the healing length $\xi = 1/\sqrt{g_{1\mathrm{D}}(\rho_0(x) - \rho_{\min})}$. Here $\rho_0(x)$ is the local background density, $\rho_{\min}$ the minimum density. The density profile of the dips is a good match to the solitonic

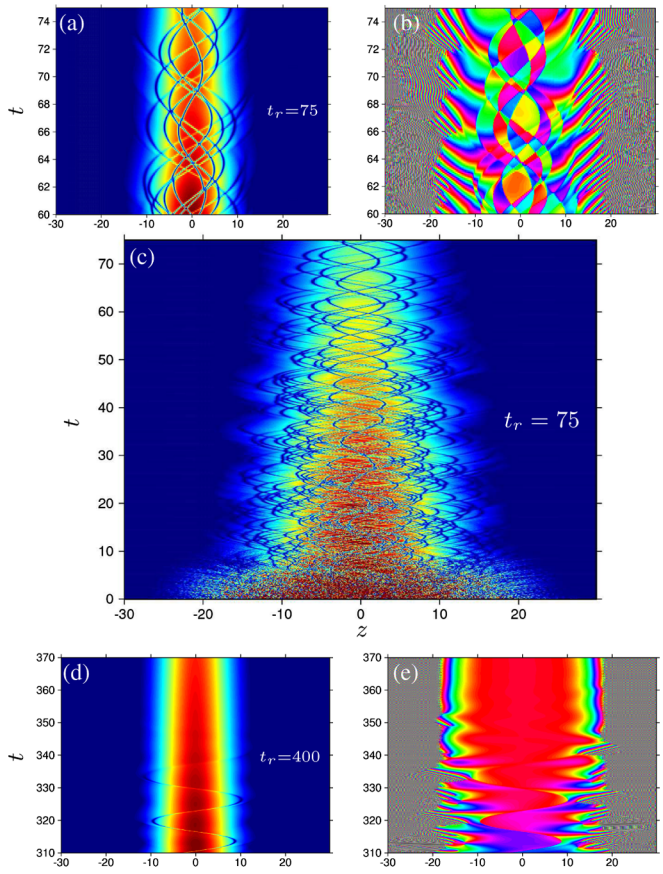

FIG. 2 (color online). Density (a),(c),(d), and phase modulo 2π (b),(e) for a single realization during the cooling ramp. In (a)–(c) $t_r = 75$ leading to a quasicondensate as $t \to \infty$, in (d),(e) $t_r = 400$ leading to a BEC. Top: at the end of evaporative cooling. Center: The entire ramp time. Bottom: the loss of the last soliton, leading to BEC formation.

solution $(\rho_{\min} + (\rho_0 - \rho_{\min})\tanh^2[(z - z_0)/\xi]$, where the dip is centered at z_0. Note the broadening of the solitons when they approach the edges of the cloud in Figs. 2(a) and 2(d). Very clear phase domains are seen between the solitons in Figs. 2(b), and account for the majority of the spatial phase variation.

As cooling progresses, many of the solitons are lost at the edges, and the size of phase domains grows. We observe that if the final state achieved is a quasicondensate (see Fig. 3), some solitons remain at t_r, while in the BEC regime (large t_r) all are already gone by this stage. Figure 3 quantifies the crossover from quasicondensate to BEC as a function of ramp time t_r.

The number of condensed atoms $N_0(t)$ is calculated from the maximal eigenvalue of the one-particle density matrix $\rho_1(z, z')$. Here, this is calculated as $\langle \psi^*(z)\psi(z')\rangle_s$, with $\langle\cdot\rangle_s$ denoting averaging over realizations within the initial canonical ensemble. The condensate fraction $n_0 = N_0/N$, is shown as the "×" data in Fig. 3. Phase correlations are characterized using the correlation function $g^{(1)}(z, z') = \rho_1(z, z')/\sqrt{\rho_1(z, z)\rho_1(z', z')}$. We use the width of the

correlation function symmetric around zero to measure the phase domain size, using: $g^{(1)}(-\frac{1}{2}l_{1/2},\frac{1}{2}l_{1/2}) = \frac{1}{2} \approx e^{-l_{1/2}/l_\phi}$. Hence, comparing to (1), $l_\phi = l_{1/2}/\log 2$.

Figure 3 shows the transition between quasicondensate and BEC behavior [2]. In the quasicondensate, the phase domain width is much smaller than the cloud, and a sizable part, or even a majority of the atoms are not condensed into the lowest energy mode. In the condensate, a single phase domain covers the entire cloud, and the condensate accounts for the vast majority of the atoms. Notably, the transition in phase correlation length $l_{1/2} = l_\phi \log 2$ around $t_r = 200$ is much sharper than in condensate fraction n_0.

As the state is nonthermal during the evolution, assigning a time-dependent temperature is moot, and we use the condensate fraction n_0 (always a well-defined quantity, unlike T) as the analogous parameter. For interpretation, several approximate results will be useful [3]: $n_0 \approx 1 - T/T_c$, when n_0 is not too close to zero, and where the characteristic temperature T_c is given by $N = T_c \log(2T_c)$. For $N = 1300$, this is $T_c = 214$. Hence, the temperature appearing in estimates of the coherence length [2,6] can be replaced by $T \to T_c(1 - n_0)$. The location of the BEC/quasicondensate transition in Fig. 3 can be compared using this T with the prediction $T_\phi = N/\mu$ [2]. The latter leads to $n_0(T_\phi) = 1 - N/(\mu T_c) \approx 0.84$, which compares favorably with the data.

To verify that the Kibble-Zurek mechanism (KZM) is at work here, we wish to compare the scaling of the number of solitons (predicted in [7]) with the rate that the characteristic temperature T_c is crossed. We count solitons by fitting the density in the solitonic solution in the same manner as in [8], using a local background density. To make the comparison, we should also calculate the quench time of the relative temperature τ_Q in which the KZM is expressed [7]. The prediction is $N_{\text{soliton}} \propto \tau_Q^{-(1+2\nu)/(1+\nu z_\tau)}$ where $\frac{dT}{dt} = -T_c/\tau_Q$, and ν and νz_τ are critical exponents for healing length and relaxation time at $T = T_c$, respectively. Here, because the system is certainly not in thermal equilibrium during the evaporative cooling phase, neither a value for T_c nor $\frac{dT}{dt}$ is forthcoming. The most reasonable straightforward estimation is that the quench time is proportional to the ramp time: $\tau_Q \propto t_r$. This leads us to use t_r as the "quench time" parameter in Fig. 4 where the scaling is examined.

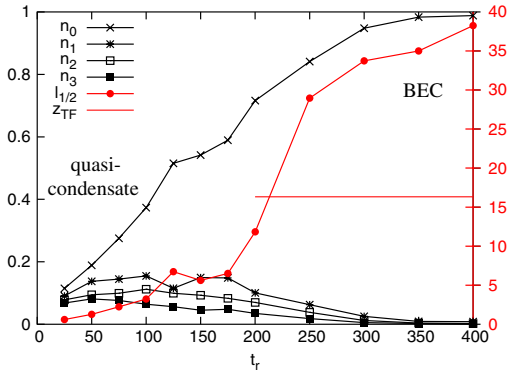

FIG. 3 (color online). Fraction of atoms in the four lowest energy modes $n_{0,1,2,3}$ (black), and phase domain width $l_{1/2}$ (red) at the end of the evaporative cooling ($t = t_r$) as a function of the ramp time t_r. The horizontal line (red) shows the Thomas-Fermi width ($2z_{\text{TF}} = 2\sqrt{2\mu}$) achieved as $t \to t_{\max}$. The ensemble consisted of 100 independent realizations. $l_{1/2} > 2z_{\text{TF}}$ occurs when phase coherence extends into the tails of the cloud.

We see that the KZM power law scaling holds quite well in the quasicondensate regime for power law exponent unity in $1/t_r$, which is the value expected for mean field [7]. As one might expect, the scaling law breaks down once the true condensate is reached for $t_r \gtrsim 200$, since the correlation length reaches or exceeds the size of the system in the BEC regime. This suppresses the slowing down near T_c that is an assumption of the KZM.

In contrast to the elongated 3D case of [7], no condensation front is apparent here. This may be an effect of the slow internal thermalization of 1D gases. We conjecture that a front might still occur in 1D if the local temperature were set externally by contact with an external reservoir, as, e.g., in buffer gas cooling, or previous work on the KZM in cold atoms [8,18].

Let us now consider the thermal equilibrium state at $t = t_{\max}$. We observe that there are indeed no solitons present. The phase domain size calculated from $g^{(1)}$ is shown by solid circles Fig. 5(e), where we also compare to the equilibrium theoretical prediction of [2] (dashed). The agreement is quite good deep in the quasicondensate regime, with a 2×–3× discrepancy for $0.5 \lesssim n_0 \lesssim 0.8$. We note that experiments also tend to show coherence lengths longer than the theoretical estimate shown [4,10].

Having calibrated our results with the two phase fluctuating situations, a connection between them can be made. We observe that the soliton creation time scale here is very short in comparison with the thermalization time. A possible hypothesis is that initial contact of coherent phase

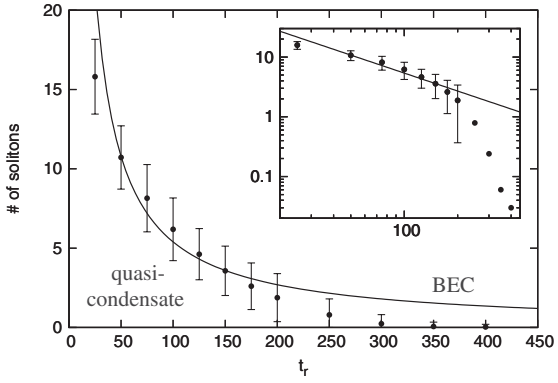

FIG. 4. The mean number of solitons at t_r (circles; error bars show standard deviation of the ensemble values). The solid line shows the scaling $N \propto 1/t_r$ approximately expected for mean-field systems from [7], fitted to the data in the quasicondensate regime ($t_r \leq 200$). The prefactor is ≈ 540. The inset shows a logarithmic scale.

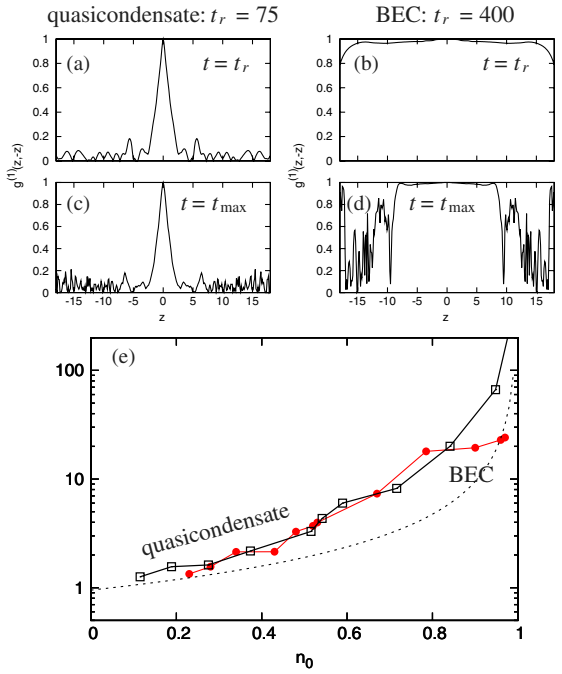

FIG. 5 (color online). Coherence length measures. (a)–(d) $g^{(1)}(z,-z)$ correlation function. (e) Phase domain widths as a function of condensate fraction n_0. Red dots: $l_{1/2}$ values at equilibrium $t = t_{max}$; open squares: d, mean distance between solitons at $t = t_r$; dashed line: stationary state prediction for $l_{1/2}$ [$l_{1/2} = l_\phi/\log 2 = (3/2z_{TF}\log 2)(N/T_c)(\frac{1}{1-n_0})$ from [2]].

domains formed via the KZM results in a soliton, which then converts into smooth phase fluctuations only on the long thermalization time scale. Such a temporal mismatch between phase and density fluctuation behavior is also reminiscent of recent experiments in ultracold helium [19]. A symptom of such a process would be to see the disappearance of solitons without change in the coherence length. Indeed, in the quasicondensate, Figs. 5(a) and 5(c) show no appreciable change from t_r to t_{max}, despite the disappearance of solitons in the meantime. A ''soliton'' measure of the phase domain size is the mean distance d between them. If phase fluctuations are ''born'' as solitons, then d at earlier times should match the final phase domain width $l_{1/2}$ in equilibrium. Figure 5 compares $d(t_r)$ at the end of the ramp with $l_{1/2}$ at equilibrium. The match is remarkably good, strongly backing up the above hypothesis that solitons can be considered the precursors or seeds of the equilibrium phase fluctuations when the gas is evaporatively cooled.

That remnants of the KZM survive in changed form into the final equilibrium state is by no means obvious. In fact, the usual procedure when investigating the KZM has been to look soon enough after the transition to catch the phase defects before they dissipate. Such transformed remnant fluctuations may also occur in other KZM situations. For example, in cosmology, if such transformed remnant fluctuations occur, they would possibly allow a new kind of indirect observation of the early Universe. For 2D gases the situation is intriguing, as defects (vortices) remain in simulations at long times [20]. We have also seen long-lived solitons under some conditions.

In conclusion, we have calculated the evaporative cooling dynamics of a 1D gas through to the quasicondensate and BEC regimes in an experimentally realistic model. The simulations confirm the action of the Kibble-Zurek mechanism for soliton formation, and their subsequent decay into long-wavelength phase fluctuations. The match between intersoliton distance at the end of the ramp and phase coherence length at long times shows that the equilibrium phase fluctuations are the transformed remnant of the solitons formed by the KZM.

We thank Wojciech Żurek, Tomasz Świsłocki, and Alice Sinatra for valuable discussions on this topic. This work was supported by Polish Government Research Funds: N N202 104136, 2009–2011 (E. W., M. G.), N N202 128539, 2010–2012 (P. D.), N N202 174239, 2010–2011 (K. R.).

[1] A. Görlitz *et al.*, Phys. Rev. Lett. **87**, 130402 (2001).
[2] D. S. Petrov, G. V. Shlyapnikov, and J. T. M. Walraven, Phys. Rev. Lett. **85**, 3745 (2000).
[3] W. Ketterle and N. J. van Druten, Phys. Rev. A **54**, 656 (1996).
[4] S. Richard *et al.*, Phys. Rev. Lett. **91**, 010405 (2003).
[5] D. Hellweg *et al.*, Phys. Rev. Lett. **91**, 010406 (2003); F. Gerbier *et al.*, Phys. Rev. A **67**, 051602(R) (2003).
[6] D. S. Petrov, G. V. Shlyapnikov, and J. T. M. Walraven, Phys. Rev. Lett. **87**, 050404 (2001).
[7] W. H. Zurek, Phys. Rev. Lett. **102**, 105702 (2009).
[8] B. Damski and W. H. Zurek, Phys. Rev. Lett. **104**, 160404 (2010).
[9] D. Kadio, M. Gajda, and K. Rzążewski, Phys. Rev. A **72**, 013607 (2005).
[10] S. Dettmer *et al.*, Phys. Rev. Lett. **87**, 160406 (2001).
[11] T. W. B. Kibble, J. Phys. A **9**, 1387 (1976); Phys. Rep. **67**, 183 (1980); W. H. Zurek, Nature (London) **317**, 505 (1985); Acta Phys. Pol. B **24**, 1301 (1993); Phys. Rep. **276**, 177 (1996).
[12] M. Brewczyk *et al.*, J. Phys. B **40**, R1 (2007).
[13] E. Witkowska *et al.*, Opt. Commun. **283**, 671 (2010).
[14] A. Sinatra *et al.*, J. Phys. B **35**, 3599 (2002).
[15] N. P. Proukakis and B. Jackson, J. Phys. B **41**, 203002 (2008).
[16] S. Manz *et al.*, Phys. Rev. A **81**, 031610(R) (2010).
[17] See supplemental material at http://link.aps.org/supplemental/10.1103/PhysRevLett.106.135301 for an animation.
[18] A. del Campo *et al.*, Phys. Rev. Lett. **105**, 075701 (2010); arXiv:1010.6190; G. De Chiara *et al.*, New J. Phys. **12**, 115003 (2010).
[19] A. G. Truscott (unpublished).
[20] C. J. Foster, P. B. Blakie, and M. J. Davis, Phys. Rev. A **81**, 023623 (2010); T. P. Simula, M. J. Davis, and P. B. Blakie, Phys. Rev. A **77**, 023618 (2008); R. N. Bisset *et al.*, Phys. Rev. A **79**, 033626 (2009); T. P. Simula and P. B. Blakie, Phys. Rev. Lett. **96**, 020404 (2006); C. N. Weiler *et al.*, Nature (London) **455**, 948 (2008).